European Journal of Pharmaceutics and Biopharmaceutics 139 (2019) 23–32

Contents lists available at ScienceDirect

European Journal of Pharmaceutics and Biopharmaceutics

journal homepage: www.elsevier.com/locate/ejpb

Research paper

Intracellular availability of poorly soluble drugs from lipid nanocapsules

Marilena Bohley, Alexandra Haunberger, Achim M. Goepferich*

Department of Pharmaceutical Technology, Faculty of Chemistry and Pharmacy, University of Regensburg, 93040 Regensburg, Germany

ARTICLE INFO

Keywords:
Lipid nanocapsules
Intracellular availability
Poorly soluble drugs
Cyclosporin A
Itraconazole
Neovascular ocular diseases

ABSTRACT

Lipid nanocapsules (LNCs) are extensively used as drug carrier systems, due to their small size distribution, biocompatibility and ease of preparation. They are especially useful for lipophilic drugs to overcome physicochemical constraints that limit their efficacy, such as low solubility in aqueous media. The aim of this work was to investigate the relationship between the intracellular availability of poorly soluble drugs delivered via LNCs and their biological efficacy in cells *in vitro*. Cyclosporin A (CsA) with a $\log P_{Oct}$ = 4.3 (Lucangioli et al., 2003) and Itraconazole (It) with a $\log P_{Oct}$ = 6.2 (Bhardwaj et al., 2013) served as model lipophilic compounds, as they are highly promising candidates for the treatment of neovascular ocular diseases. Due to their lipophilic properties and the resulting preference for the oily core of LNCs, high encapsulation efficiencies were achieved. Drug-loaded LNCs with particle sizes around 50 nm were grafted with an αvβ3 integrin ligand (RGD) to optimize cellular uptake by human dermal microvascular endothelial cells. Even though RGD-LNCs showed excellent internalization, they exhibited insufficient inhibitory effects *in vitro* regarding endothelial cell proliferation, vascular endothelial growth factor expression, and tube formation in contrast to free drugs. This loss of efficacy could be explained by negligible intracellular availability of the poorly soluble drugs from LNCs.

1. Introduction

Lipid nanocapsules (LNCs) are widely used as delivery systems, especially for poorly soluble drugs. This extensive use can be explained by their narrow size distributions with achievable sizes between 25 and 100 nm, biocompatible nature, simplicity of preparation, and capacity to encapsulate a broad range of drugs with various solubility characteristics [1]. LNCs usually consist of an oily core made of medium-chain triglycerides, surrounded by a mixture of lecithin and a PEGylated surfactant. Their formulation is commonly based on the phase-inversion temperature phenomenon of emulsions leading to LNC formation with good mono-dispersity [2]. In light of these advantages, we have chosen LNCs as a delivery system for lipophilic antiangiogenic drugs for the treatment of neovascular ocular diseases.

Neovascular ocular diseases, in particular exudative age-related macular degeneration (wet AMD) and proliferative diabetic retinopathy (DR), are associated with pronounced choroidal or intraretinal neovascularization, during which the blood vessels become leaky and begin to sprout [3]. With the observation that blood vessel proliferation and hyperpermeability are the major underlying pathomechanisms [4,5], vascular endothelial growth factor (VEGF) was identified as a key regulator of these processes [6,7]. Currently, VEGF is well known to be of paramount significance for the regulation of angiogenesis [8], blood vessel permeability, and the creation of endothelial cell fenestrations [9,10]. As a consequence, today's standard therapy for the treatment of neovascular ocular diseases are intravitreal anti-VEGF antibody injections [11]. Even though this therapeutic concept has shown great success, there are numerous drawbacks and side effects that accompany continuous anti-VEGF therapy. Blocking the VEGF signaling pathway completely results in blocking all the positive VEGF effects as well [12]. The biological VEGF effects in the retina are not limited to endothelial cells, where the effects are undesired, because VEGF receptors are expressed on a number of other cell types such as Müller cells, astrocytes, photoreceptors, and retinal pigment epithelial cells [13,14]. Clinically, rigorous suppression of omnipresent VEGF levels manifests in a decrease of choroid thickness [15]. Epidemiologically, the risk of contracting geographic atrophy increases under long-term anti-VEGF antibody therapy, and is accompanied by massive local cell death of retinal pigment epithelium cells and photoreceptors [16].

With AMD and DR being two of the leading causes of blindness globally [17,18] and the limitations of continuous and rigorous VEGF knockdown in the retina, there is an urgent need for the development of new therapeutic concepts. Therefore, we developed antiangiogenic drug-loaded LNCs that allow for choroidal endothelium-specific anti-VEGF therapy. Ideally, this therapy would spare all cell types in the retina that suffer from general VEGF deprivation. Therefore, αvβ3

* Corresponding author.
E-mail address: achim.goepferich@ur.de (A.M. Goepferich).

https://doi.org/10.1016/j.ejpb.2019.03.007
Received 12 December 2018; Received in revised form 14 February 2019; Accepted 5 March 2019
Available online 07 March 2019

integrins were chosen as a promising target for selective nanoparticle delivery, because their expression is limited to very few cell types and they are significantly over-expressed during neovascularization [19]. In the case of αvβ3 integrin, it is preferentially expressed by proliferating endothelial cells [20–22]. Additionally, integrins stand out due to their high rates of receptor-mediated endocytosis, which could facilitate the intracellular delivery of targeted nanoparticles [23,24].

Therefore, the highly potent and αvβ3 integrin-specific ligand cyclo (Arg-Gly-Asp-D-Phe-Cys) (RGD) was attached to the LNC surface to target proliferating endothelial cells [25,26]. For intracellular anti-VEGF therapy, two highly appealing drugs were chosen: Cyclosporin A (CsA) and Itraconazole (It). They are already well known and widely used as an immunosuppressant and an antifungal drug, respectively. Besides their current scope of application, both interfere with the VEGF signaling pathway at different intracellular sites.

CsA is able to suppress the intracellular VEGF signaling pathway [27] and alleviates endothelial cell sprouting and proliferation *in vitro* [28,29]. Additionally, CsA counteracts the TGFβ-related increase of VEGF production in retinal pigment epithelial cells [30], which is the main source of VEGF in the retina [31]. Furthermore, CsA possesses anti-inflammatory potential and decreases interleukin-1β levels. In addition, CsA repairs damage to the blood-retina-barrier in an animal model of diabetes [32]. VEGF receptor type 2 (VEGF-R2) glycosylation and intracellular trafficking is not only inhibited by CsA, but also by It [33], and the same applies to endothelial cell proliferation [34]. According to Nacev et al., the drugs exert synergistic effects [28].

CsA has been shown to significantly, but moderately alleviate progression of diabetic retinopathy after oral administration to transplantation patients, demonstrating its high therapeutic potential but suffer from an insufficient availability in the ocular vasculature [35–37].

We have designed targeting nanocarriers loaded with CsA and a combination of CsA and It to overcome this lack of intracellular availability and concomitantly reduce side effects. The aim of this work was to elucidate whether an appropriate intracellular availability of CsA and It could be achieved by using LNCs as carrier systems for the poorly soluble drugs. The intracellular availability was investigated by comparing the inhibitory efficacy of CsA and a combination of CsA and It encapsulated in LNCs or as free drugs, on endothelial cell proliferation, VEGF-receptor expression, and tube formation.

2. Materials and methods

2.1. Materials

Cyclosporin A (CsA) was obtained from Pharma Stulln GmbH (Stulln, Germany). Itraconazole (It) was purchased from Fagron GmbH (Barsbüttel, Germany). Kolliphor® HS15 was obtained from BASF. Lipoid® S75-3 was obtained from Lipoid GmbH (Ludwigshafen, Germany). Miglyol® 812 (MCT) was purchased from Caesar & Loretz GmbH (Hilden, Germany). NaCl was obtained from Merck (Darmstadt, Germany). 3,3′-Dioctadecyloxacarbocyanine perchlorate (DiO) and 1,1′-Dioctadecyl-3,3,3′,3′-Tetramethylindocarbocyanine perchlorate (DiI) were purchased from Invitrogen (Thermo Fisher Scientific, Waltham, MA, USA). Purified water was obtained from a MilliQ System from Millipore (Schwalbach, Germany). Dulbecco's phosphate buffered saline (DPBS) was obtained from Gibco® Life Technologies (Thermo Fisher Scientific, Waltham, MA, USA). Cyclosporine D (CsD) was a generous gift from Prof. Dr. F. Kees (University of Regensburg, Germany). Methanol and dichloromethane, analytical standard, were purchased from Merck (Darmstadt, Germany). 1,2-Distearoyl-*sn*-glycero-3-phosphoethanolamine-N[maleimide(polyethyleneglycol)-2000] (ammonium salt) (DSPE-PEG2000-maleimide) and 1,2-Distearoyl-*sn*-glycero-3-phosphoethanolamine-N-[methoxy(polyethylene glycol)-2000] (ammonium salt) (DSPE-mPEG2000) were purchased from Avanti Polar Lipids Inc. (Alabaster, AL, USA) and cyclo(Arg-Gly-Asp-D-Phe-Cys) acetate salt (RGD) from Bachem Distribution Service GmbH (Weil a. Rhein, Germany).

Fetal Calf Serum (FCS) was purchased from Biowest (Nuaillé, France). Recombinant Human Vascular Endothelial Growth Factor (VEGF)-165, APC anti-human CD309 (VEGF-R2) Antibody and APC Mouse IgG1, κ Isotype Ctrl Antibody were obtained from BioLegend UK Ltd. (London, UK). 3-(4,5-Dimethyl-2-thiazolyl)-2,5-diphenyl-2H-tetrazolium bromide (MTT) and sodium dodecyl sulfate (SDS) were purchased from AppliChem (Darmstadt, Germany). Leibovitz's L-15, Trypsin-EDTA (0.25%) and Calcein-AM were obtained from Life Technologies (Thermo Fisher Scientific, Waltham, MA, USA). Propidium iodide was purchased from Sigma-Aldrich (Taufkirchen, Germany). Matrigel® Matrix was obtained from Corning (Amsterdam, Netherlands).

2.2. Cell culture

Human dermal microvascular endothelial cells (HDMECs) were purchased from PromoCell GmbH (Heidelberg, Germany) and cultured in endothelial cell growth medium MV (GM) and endothelial cell basal medium MV (BM), purchased from PromoCell GmbH (Heidelberg, Germany). HDMECs were exclusively used in low passage numbers ranging from 4 to 6. Furthermore, it was ensured that confluence levels were below 80% in every experiment.

2.3. Preparation of lipid nanocapsules

LNCs were prepared according to a modified protocol originally based on the work of Heurtault et al. [2]. In short, 887.5 mg Kolliphor® HS15, 30 mg Lipoid® S75-3, 415 mg MCT, 12 mg NaCl and 655.8 mg water were subjected to three cycles of progressive heating and cooling between 90 and 60 °C. To quantify particles after modification and purification, fluorescent dyes (DiI or DiO 1.5% (w/w)) were added to the initial mixture. During the last cycle, an irreversible shock was induced by dilution with 5 ml water at the phase inversion temperature, leading to the formation of stable LNCs. Afterwards, additional magnetic stirring was applied for 5 min at room temperature. The final dispersion was filtered through a 0.22 µm regenerated cellulose (RC) membrane for sterilization and stored at room temperature in the dark.

To prepare drug-loaded LNCs, 35.3 mg CsA were dissolved in MCT and particles were prepared as described above. For It encapsulation, 0.1 mg was dissolved in dichloromethane and added to the mixture of MCT, Kolliphor, Lipoid, and NaCl. Dichloromethane was then evaporated at 75 °C for 30 min. Afterwards, the water was added, and the first heating cycle was initiated.

2.4. Drug loading studies

Free non-encapsulated drug was separated from the LNCs by ultrafiltration using an Amicon® Ultra-4 MWCO 10 kDa centrifugal filter (Merck, Germany), as described previously [38,39]. 2 g of freshly prepared LNC dispersion were centrifuged for 30 min at 4000*g*. The resulting filtrate was weighed, and the retentate weight adjusted to 2 g with water. After that, 20 µl of sample was diluted 5000-fold with methanol and ultrasonicated for 30 min to disrupt the particles and extract the drug, which was quantified by UHPLC-MS, as previously described [40]. Briefly, CsD was used as an internal standard, and a calibration curve was made with CsA in blank LNC methanol solution, prepared as described above. Samples were analyzed in triplicate and the mean ± SD was calculated (mg of CsA per g of LNC dispersion). The encapsulation efficiency was determined (experimental drug payload/theoretical drug payload).

2.5. RGD-Peptide grafting on LNCs

First, peptides were coupled to the amphiphilic DSPE-PEG2000-maleimide using conjugation chemistry between the thiol group present

on the cyclic structure of the peptide and the maleimide [41]. Next, the conjugate or DSPE-mPEG2000 was inserted in the shell of the LNCs by post-insertion method [42]. Modified LNCs were dialyzed against DPBS overnight using Spectra/Por® Float-A-Lyzer® G2 MWCO 300 kDa (Sigma-Aldrich, Germany) and subsequently centrifuged twice (15 min, 4000*g*) using an Amicon® Ultra-4 MWCO 100 kDa centrifugal filter (Merck, Germany) for further purification.

2.6. Characterization of LNCs

Dynamic light scattering (DLS) was used to determine the Z-average particle diameter and the polydispersity index (PDI) of LNCs using a Zetasizer®Nano ZEN 3600 (Malvern Instruments, Worcestershire, UK). All batches were diluted in 10% DPBS and were analyzed in triplicate.

2.7. In vitro experiments

2.7.1. Cellular uptake studies

Flow Cytometry studies were performed on 24-well plates using DiO-labeled LNCs. 50000 cells/well were seeded and incubated overnight in GM. GM was then aspirated, the cells were washed with DPBS and afterwards incubated with different LNC dispersions (0.6 mg/ml) for 45 min at 37 °C. The cells were then washed with DPBS, detached from the well surfaces, washed again and re-dispersed in DPBS. Immediately prior to the measurement they were stained with propidium iodide to exclude damaged cells during analysis. The cells were analyzed using a BD FACS Calibur™ fluorescent-activated flow cytometer with BD CellQuest™ software (BDBiosciences, Heidelberg, Germany). Fluorescence was excited at 488 nm and recorded with a FL1 530/30 (DiO-LNCs) bandpass filter and a FL3 670 nm (PI) long pass filter. 10000 cells were measured in each sample and untreated cells were used as internal control. Data was analyzed with Flowing Software (Turku Centre of Biotechnology, Finland). The population of viable cells was gated, and the mean fluorescence intensity was analyzed.

For Confocal Laser Scanning Microscopy, 20000 cells/well were seeded in 8-well µ-slides (ibidi, Planegg, Germany) and incubated overnight. Cells were washed with DPBS, LNC samples (0.6 mg/ml) were added and incubated for 45 min at 37 °C. Afterwards, cells were washed twice, covered with Leibovitz's Medium supplemented with 10% FCS and examined with a confocal microscope LSM 510 Meta (Zeiss, Oberkochen, Germany), using a Plan-Apochromat 63 × /1.4 oil objective. Fluorescence was excited at 488 nm with an argon laser, and emission was recorded with a 505 nm long pass filter. Images were captured and analyzed using ZEN (Zeiss, Oberkochen, Germany).

2.7.2. MTT assay

To determine cellular proliferation and viability, the MTT assay after Mosmann and Buttke et al. [43,44] was adapted. In short, 4000 cells/well were seeded in 96-well plates and incubated overnight to allow the cells to adhere. Then the GM was replaced by various dilutions of VEGF (5–100 ng/ml), CsA (1.0–25 µg/ml), It (0.1–2.5 µg/ml), CsA/It in a ratio of 10:1 (1.0/0.1–25/2.5 µg/ml), CsA RGD-LNC, CsA + It RGD-LNC, or RGD-LNC (0.6 g/ml) in BM supplemented with 2% FCS. The cells were incubated at 37 °C for 24 h, and then drug-containing medium was removed, and the cells were washed with DPBS. 0.63 mg/ml MTT solution (in 75% GM and 25% DPBS) was added to each well with a subsequent incubation over 4 h. Afterwards, MTT solution was aspirated carefully and 10% SDS solution was added. The cells were further incubated overnight in the dark at room temperature. Lastly, the degree of proliferation was ascertained by measuring the absorbance at 570 nm on a microplate reader (FLUOstar Omega, BMG Labtech). Absorbance values were used to calculate the proliferation rate by referring to untreated control cells with a proliferation value of 100%.

2.7.3. Cell cycle analysis

Cell Cycle Analysis by flow cytometry was performed as previously described [45–48], to determine the percentage of cells in the $G_{0/1}$-, S- and G_2- Phases after DNA staining with propidium iodide. In short, 1 million cells were seeded in T75 culture flasks and incubated in GM overnight. Afterwards the GM was aspirated, the cells were washed with DPBS and samples (25 µg/ml CsA, 1.0/0.1 µg/ml CsA/It and 0.6 mg/ml CsA RGD-LNCs or CsA/It RGD-LNCs) in BM with 10 ng/ml VEGF were added. After an incubation period of 24 h, the samples were aspirated, the cells were washed, pelletized and washed twice again. 1 million cells per sample were transferred to a falcon tube, centrifuged again, resuspended in DPBS, and stored on ice for 5 min. Next, methanol was added under continuous stirring to dilute samples to 70% methanol and the cells were fixed for a minimum of 12 h. After the fixation process, the cells were washed with DPBS again and resuspended in 425 µl DPBS. 50 µl RNAse (Qiagen, Venio, Netherlands) (1 mg/ml) were added and incubated at 37 °C for 20 min. Thereafter 25 µl propidium iodide (1 mg/ml) were added and samples were measured by flow cytometry with 50000 counts/sample. Fluorescence was excited at 488 nm with an argon laser and emission was recorded with a FL3 670 nm (PI) long pass filter. Analysis and quantification were performed using ModFit LT (Verity Software House, Maine, USA).

2.7.4. VEGF-receptor-2 expression

To investigate the effect of drug-loaded LNCs and free drugs on VEGF-R2 expression, flow cytometry was used. For that 50000 cells/well were seeded in a 24-well plate and grown in GM overnight. Thereafter, the cells were washed with DPBS and samples (25 µg/ml CsA, 1.0/0.1 µg/ml CsA/It and 0.6 mg/ml CsA RGD-LNCs or CsA/It RGD-LNCs) in BM containing 10 ng/ml VEGF were added and incubated for 24 h. Then, they were washed again, pelletized, and resuspended in cell staining buffer (DPBS supplemented with 5% FCS). APC anti-human CD309 (VEGF-R2) Antibody and APC Mouse IgG1, κ Isotype Ctrl Antibody were added to untreated and treated cells. After an incubation of 20 min on ice in the dark, the cells were pelletized again and washed twice with cell staining buffer before analysis. 10000 events per sample were measured using flow cytometry. Fluorescence was excited at 635 nm, and emission was recorded with a FL4 661/8 nm (APC) bandpass filter. Data was analyzed by using mean fluorescence intensity, excluding mean fluorescence values obtained by isotype control, using Flowing Software (Turku Centre of Biotechnology, Finland).

2.7.5. Tube formation assay

Tube formation assays were performed to test antiangiogenic potency [49] of drug-loaded RGD-LNCs and free drugs on HDMECs, according to previously published methods [50]. Briefly, a 96-well plate was coated with 50 µl Matrigel® per well. HDMECs were stained with Calcein-AM and adjusted to 1 million cells/ml. 1 ml of cell dispersion per sample was pelletized in Eppendorf tubes, resuspended in 25 µg/ml CsA, 1.0/0.1 µg/ml CsA/It and 0.6 mg/ml CsA RGD-LNCs or CsA/It RGD-LNCs and 10000 cells/well were seeded gently on Matrigel®. The cells were examined after 2, 4, 6, 8, 10, and 24 h for tube formation using an inverted microscope LSM 510 Meta (Zeiss, Oberkochen, Germany) with a 5× objective, 488 nm laser, Ph1 (phase contrast). Quantification of tube networks was performed by using Angiogenesis Analyzer for ImageJ [51]. As quantification parameters, the percentage reduction of nodes and the total tube length were used.

2.7.6. Statistical analysis

All data are indicated as means ± SD of at least three independent experiments. The statistical analysis was performed using GraphPad Prism 6 and by using one-way ANOVA (unless otherwise stated). Significant differences were indicated as: *($P < 0.05$), **($P < 0.01$), *** ($P < 0.001$) and **** ($P < 0.0001$) related to control unless otherwise stated.

Table 1
Zeta potential [mV], drug payload [mg/g LNC dispersion] and encapsulation efficiency [%] with standard deviation of three independent batches. Drug payload and encapsulation efficiency characterized by HPLC-MS with a correlation coefficient $r^2 = 0.995$.

	Drug payload [mg/g LNC]	Encapsulation efficiency [%]	Zeta Potential [mV]
CsA LNCs	34.1 ± 0.7	66.8 ± 1.2	−2.26 ± 0.73

3. Results

3.1. Drug loading studies

The poorly water-soluble drug CsA was dissolved in the oil phase prior to preparation. High encapsulation efficiencies were achieved with values of 67% and a drug payload of 34.1 mg/g LNC (Table 1). Similar behavior can be expected for It, due to its even lower water solubility compared to CsA [52,53].

No significant differences could be detected in terms of drug payload and encapsulation efficiency between the batches, indicating that the manufacturing process of drug-loaded LNCs is very reproducible. Nevertheless, there is a considerable amount of non-encapsulated CsA that presumably does not appear in a free state in the aqueous phase because there were no detectable amounts of free CsA in the filtrate after purification (data not shown).

3.2. Particle characterization

It is well known that particle size is a key factor in cellular uptake of nanoparticles and that uptake increases with decreasing particle diameter up to an optimal point. In general, for nanoparticles with diameters below 100 nm, good cellular uptake has been shown, while the optimal size for cellular internalization seems to be 50 nm [54]. Although, the size is only one factor that affects cellular internalization of nanocarriers [55]. Another important physicochemical property regarding cellular uptake is the surface charge. Increased cellular internalization can be achieved by an enhancement of surface charge, either positive or negative, while extensive charges might lead to lysosomal escape or lysosome co-localization [56]. Based on this knowledge, we prepared LNCs with a diameter of approximately 50 nm and a slightly negative zeta potential.

Size and polydispersity index (PDI) of blank LNCs as well as peptide-grafted LNCs are presented in Fig. 1. Encapsulation of drugs or dyes did not change these characteristics (data not shown), as described by others [57]. On the contrary, DSPE-mPEG or DSPE-PEG-RGD inserted after encapsulation increased the size of LNCs by an average of 10 nm, while PDI remained relatively low, indicating effective attachment of the peptides. For all formulations, the polydispersity index was < 0.07,

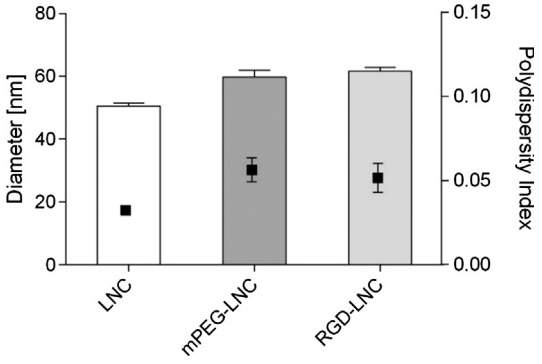

Fig. 1. Size (bars) and size distribution (polydispersity, black squares) measured in 10% DPBS at 25 °C.

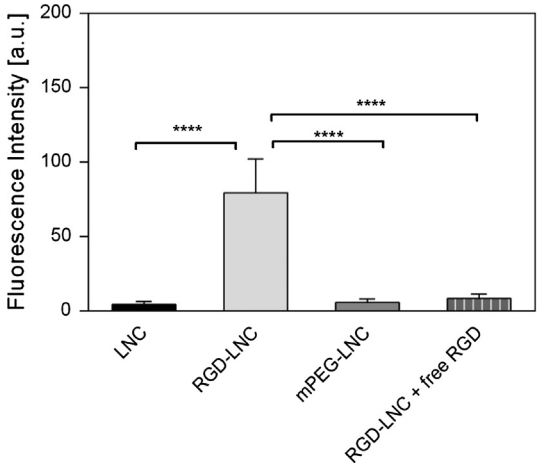

Fig. 2. Mean fluorescence intensity of cells incubated with 0.6 mg/ml of modified, DiO loaded LNCs for 45 min incubation time at 37 °C.

which demonstrates narrow size distributions of all preparations.

3.3. Cellular uptake studies

Internalization of modified and unmodified LNCs was evaluated *in vitro* by using flow cytometry (FACS) (Fig. 2) and confocal microscopy (Supplements S1). The FACS analysis revealed excellent cellular uptake of RGD-LNCs, whereas uptake of unmodified LNCs or mPEG-LNCs was negligible. The significantly higher internalization of RGD-LNCs confirmed the interaction between the RGD peptide and $\alpha_v\beta_3$ integrins on the cell surface of endothelial cells, as previously reported [58]. This is additionally supported by the fact that there is a significant decrease of the fluorescent values when free RGD is added and $\alpha_v\beta_3$ integrins are saturated with free ligand. This clearly demonstrates active uptake of RGD-LNCs via $\alpha_v\beta_3$ integrin receptors and reveals that a targeting ligand on the shell of LNCs is needed to achieve satisfactory internalization.

Confocal laser scanning microscopy (CLSM) was used to confirm the excellent cellular uptake revealed by FACS analysis and to determine whether the LNCs were cell-surface bound or internalized. The CLSM pictures confirmed the results from the flow cytometry experiments (Supplements S1). Like the untreated cells (A), cells treated with LNCs (B) or mPEG-LNCs (D) showed no measurable fluorescence. Dense, bright fluorescence can be observed in the cytosolic region of the cells treated with RGD-LNCs (excluding the nucleus which showed less fluorescence) (C). This suggests that the RGD-LNCs were internalized rather than bound to the cell membrane. The internalization of RGD-LNCs was inhibited by the addition of free RGD during the incubation, indicating specific receptor-mediated uptake (E).

With both standard methods for the investigation of cellular uptake, we found that RGD-LNCs can interfere functionally with the $\alpha_v\beta_3$ integrin *in vitro*. This indicates that the coupling and post-insertion process was successful and resulted in efficient recognition of the integrin receptors on the cell surface. Additionally, the results show that a targeting ligand is essential for achieving a sufficient uptake of LNCs, as non-modified LNCs were not taken up into the cells. Furthermore, the results reflect the great potential of RGD-LNCs for effectively and specifically delivering drugs into endothelial cells. Contrary to previous findings in the literature, we could not detect that LNCs or mPEG-LNCs were actively or passively internalized by cells with the experimental conditions we used [59,60].

3.4. Evaluation of cell proliferation

Firstly, an MTT assay was used to determine the ability of CsA and It

to hamper cell proliferation *in vitro* both in the presence and absence of VEGF. VEGF is a growth factor with high angiogenic potential due to its stimulation of endothelial cell proliferation and its inhibition of endothelial cell apoptosis [61]. Therefore, the effect of different concentrations of free drugs (CsA, It, It + CsA) with and without addition of VEGF on HDMECs was investigated. Performing the same experiment with and without growth factor revealed whether the inhibitory effects of CsA and It are VEGF-dependent.

To determine the optimum VEGF concentration for HDMECs, different concentrations were used (supplements S2). We found that 10 ng/ml was the most effective VEGF concentration for cell proliferation, which is in accordance with previous findings [62]. This concentration was subsequently used in all other *in vitro* experiments.

Interestingly, we saw that freshly prepared, drug free, unmodified LNCs showed major toxic effects on HDMECs (supplements S3). This toxicity could be avoided by using the same purification processes used after post-insertion of the targeting peptide, indicating that toxicity was probably due to free components from the manufacturing process, which could be removed by dialysis and centrifugation.

The ratio of CsA to It was kept at 10:1, as it has been shown to be the ratio with the highest synergistic effect according to Nacev et al. [28].

All treatment groups showed dose dependent inhibition profiles (Fig. 3). Especially in the case of free CsA the inhibitory effect on cell proliferation is greater in the presence of VEGF, indicating, that there is a massive VEGF-dependency of the CsA efficacy.

CsA 25 (25 μg/ml) represents the greatest possible loading that can be reached in LNCs containing MCT as the oily core when using LNC concentrations of 0.6 mg/ml for *in vitro* experiments. With these conditions, it is excellent to see that there is such a strong reduction in proliferation, especially when VEGF is present. In the case of free It, our observations were similar. There is dose dependence, and the inhibitory effects on cell proliferation are also greater in the presence of VEGF, so it can be assumed that It acts in a VEGF-dependent manner as well. However, only 0.1 mg It could be encapsulated in the LNCs, resulting in a concentration of approx. 0.1 μg/ml It when using 0.6 mg/ml LNC dispersion. Still, we investigated the effects of 1.0 μg/ml It and 2.5 μg/ml It on cell proliferation as well, to determine if higher loading would reveal in higher efficacy. Nevertheless, in the presence of VEGF, 1.0 μg/ml It showed a statistically significant inhibitory effect on the proliferation rate.

Statistically significant inhibitory effects and dose dependency could also be seen for the combination of both drugs. Paradoxically, the observed extent of inhibition is, in the case of combining both drugs, stronger when there is no VEGF present. Unfortunately, the previously described [28] synergistic effect of combined CsA and It did not beat the efficacy of higher concentrations of CsA used alone. With these results, CsA 25 was selected as the most promising concentration, which was used in comparison with CsA 1.0/It 0.1. This combination of the two drugs in a 10:1 ratio represents the highest possible concentration achievable.

Having confirmed that free CsA and CsA combined with It inhibit HDMEC proliferation and that these cells take up RGD-LNCs, we loaded these drugs into LNCs and tested them for their inhibitory effects on cell proliferation (Fig. 4).

The MTT assay was performed using the same protocol as that used to evaluate the inhibitory potential of free CsA and It but yielded different results. CsA RGD-LNCs and It + CsA RGD-LNCs induced significant decreases in proliferation rate compared to the untreated control, but to smaller extends than free drug. Free CsA decreased the proliferation rate by 50%, while CsA RGD-LNCs only achieved a reduction of 20%. The degree of inhibition caused by It + CsA RGD-LNCs was minor, with no statistically significant differences from RGD-LNCs or CsA RGD-LNC. In contrast, the inhibitory efficiency of CsA RGD-LNCs was significant compared to RGD-LNCs. Drug-free RGD-LNCs showed no effect on the proliferation rate, confirming the cytocompatibility of the particles, as observed previously (supplemental information S3). Unexpectedly, free CsA had a highly efficient inhibitory effect on the proliferation rate of HDMECs but loading it into RGD-LNCs caused a loss of efficiency. The same trend could be seen for the combination of both drugs, despite the effects of free combined drugs being lower anyway.

3.5. Cell cycle analysis

To confirm the results of the MTT assay with another independent method, cell cycle analysis was performed to determine the inhibitory effect on cell proliferation of drug-loaded RGD-LNCs. To this end, flow cytometry was used to monitor the nuclear content of a cell and its changes during proliferation [48]. The goal was to determine whether RGD-LNCs loaded with CsA or the combination of It + CsA were able to decrease the amount of cells in the S-phase, when DNA is replicated, and trap these cells in the $G_{0/1}$-phase [63]. Accordingly, HDMECs were incubated with free drugs or drug-loaded RGD-LNCs as in the MTT assays.

Fig. 5A shows the overlay graphs of all phases of the cell cycle. There was a slight increase in the number of cells in the $G_{0/1}$-phase for CsA and It loaded RGD-LNCs. Free CsA showed the highest increase of cells in the $G_{0/1}$-phase. There were no significant differences among samples regarding the G_2/M-phase. Fig. 5B gives more detailed insight into the S-phase, as the proportion of cells in this phase gives the most relevant readout. CsA-loaded RGD-LNCs had a statistically significant effect on cell cycle distribution, although they did not reach the efficacy of free CsA.

These results match the results obtained from the MTT assay, indicating that the efficacy of drug-loaded RGD-LNCs lags behind that of free drugs, despite RGD-LNCs having excellent targeting to and internalization in HDMECs (see Fig. 2 and Supplements S1). An explanation for this phenomenon could be poor intracellular bioavailability of the drugs from the LNCs, due to their high lipophilicity and solubility in the oily core. It cannot be due to the drugs, because they revealed excellent biological effects when dissolved in DMSO.

3.6. VEGF-receptor-2 expression

VEGF-Receptor 2 (VEGF-R2) mediates the biological effects of VEGF, which is well known as a key regulator of pathological angiogenesis [64]. Reduction on the expression levels of VEGF-R2 has been discovered for both CsA and It [27,34]. To determine if free drugs or drug-loaded RGD-LNCs can reduce VEGF-R2 expression, we made *in vitro* evaluations with HDMECs and anti-human CD309 (VEGF-R2) antibody. Nonspecific binding of the CD309 antibody was investigated by using mouse IgG1 antibody as the isotype control. Fluorescence values resulting from non-specific binding were subtracted from all samples, including untreated cells.

Fig. 6 displays that unloaded RGD-LNCs did not change VEGF-R2 expression values, as would be expected. Free CsA again reveals great efficacy, as it is able to eliminate expression almost completely. On the contrary, expression levels seemed to increase after treatment with drug-loaded RGD-LNCs, but not significantly compared to control.

This shows once again that CsA at the chosen concentration is a highly promising drug candidate for the treatment of neovascular diseases and that CsA encapsulation in LNCs leads to a massive loss of efficacy. For the combination of both drugs, similar observations could not be made. This is probably due to the low concentrations (0.1 μg/ml It and 1.0 μg/ml CsA) used, as even the free drugs showed no statistically relevant effect on VEGF-R2 expression.

3.7. Tube formation assay

Besides cell proliferation and VEGF-receptor expression, *in vitro* angiogenesis can be assessed by the tube formation assay [27]. This assay has the highest explanatory power regarding the process of

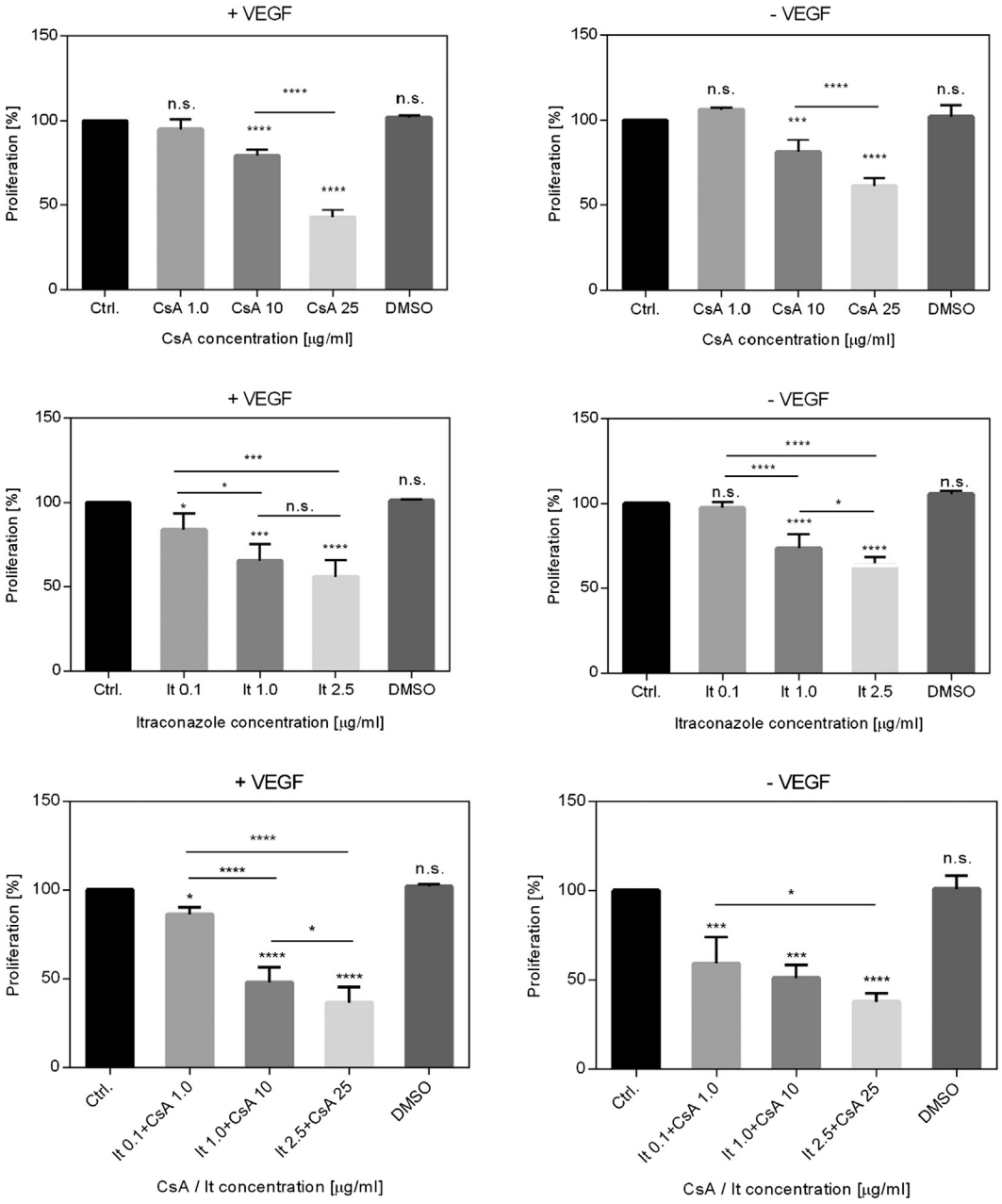

Fig. 3. MTT assay showing the proliferation rate (%) relative to untreated cells as control. All experiments were carried out with HDMECs that were incubated for a 24 h period. Drugs were dissolved in DMSO, which was used as a control in the experiments. Cells were incubated with 1.0, 10, 25 µg/ml CsA, 0.1, 1.0, 2.5 µg/ml It, and It 0.1 + CsA 1.0, It 1.0 + CsA 10, It 2.5 + CsA 25 µg/ml. All experiments were performed with and without addition of 10 ng/ml VEGF.

angiogenesis besides *in vivo* experiments. The tube formation assay involves not only one parameter like proliferation rate or receptor expression, but the complex interaction of different processes within cells while building new structures, including cell adhesion, migration, protease activity, and tubule formation [65]. When HDMECs were seeded on a matrix, they built capillary-like structures (tubes) within a time frame of 24 h, with a maximum reached after 8 h of incubation (Fig. 7).

Free CsA exhibited marked inhibitory effects on the formation of tube-like structures by HDMECs, visible by significant reduction of the number of nodes and total tube length compared to untreated cells (Fig. 8). Drug-free RGD-LNCs showed no influence on the tube formation, as expected. Contrary to what would be expected, drug-loaded RGD-LNCs (CsA RGD-LNC and It + CsA RGD-LNC) had no effect on the tube formation. The combination of both free drugs revealed a slight effect on the number of nodes, whereas there was no detectable effect on the total tube length.

These results displayed a lack of inhibitory potential of drug-loaded RGD-LNCs on tube formation of HDMECs. This correlates with our previous experiments and shows that the anti-angiogenic potential of free drugs is lost once they are incorporated into this nanoparticle system. We hypothesize that the high lipophilicity of both drugs and their dissolution in the lipophilic core of the nanoparticle lead to poor intracellular availability and concomitant loss of biological efficacy.

4. Discussion

In this study, anti-angiogenic effects of CsA- or CsA + It-loaded in RGD-grafted LNCs were assessed *in vitro* using proliferating microvascular endothelial cells. We could demonstrate that targeted RGD-LNCs showed optimal physicochemical properties regarding size, PDI, and encapsulation efficiency, as well as excellent cellular uptake upon

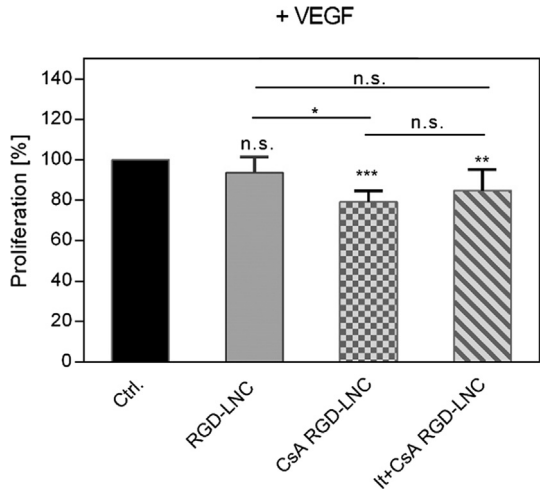

Fig. 4. MTT assay showing the proliferation rate (%) relative to untreated cells as control. HDMECs were incubated for a 24 h period with either 0.6 mg/ml of targeted RGD-modified LNCs (RGD-LNCs), CsA-loaded RGD-LNCs (CsA RGD-LNC), or It- and CsA-loaded RGD-LNCs (It + CsA RGD-LNCs).

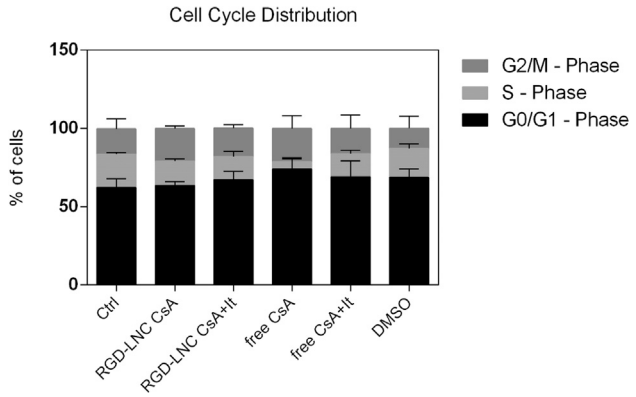

Fig. 5A. Cell cycle distribution for HDMECs using 25 µl propidium iodide (1 mg/ml) and 50 µl RNAse (1 mg/ml) for DNA-staining. HDMECs were treated with 10 ng/ml VEGF with addition of free CsA (25 µg/ml), free CsA + It (1.0 + 0.1 µg/ml), 0.6 mg/ml CsA-loaded RGD-LNCs (CsA RGD-LNC), or 0.6 mg/ml CsA- and It-loaded RGD-LNCs (CsA + It RGD-LNCs) for 24 h at 37 °C. Free drugs were dissolved in DMSO, which was used as a control in the experiments.

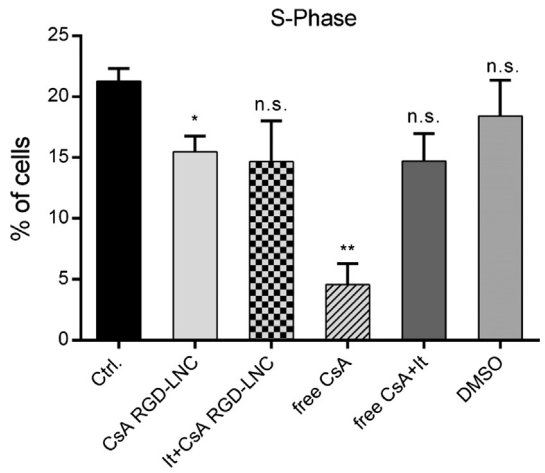

Fig. 5B. Further Analysis of the average S-phase fraction, referring to Fig. 5A.

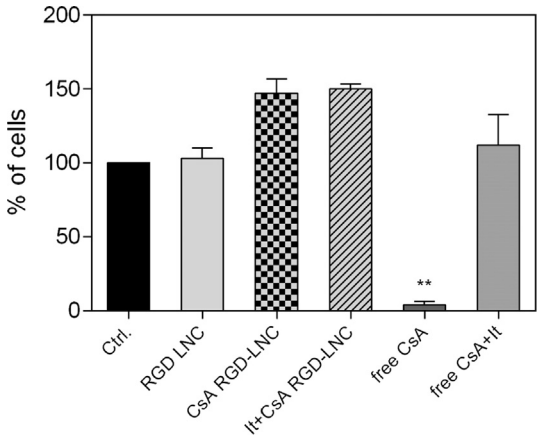

Fig. 6. Expression of VEGF-R2 in HDMECs, stained with anti-human CD309 (VEGF-R2) antibody. Effects of free CsA (25 µg/ml), free CsA + It (1.0 + 0.1 µg/ml) and 0.6 mg/ml drug-free RGD-LNCs, 0.6 mg/ml CsA-loaded RGD-LNCs (CsA RGD-LNC) or 0.6 mg/ml CsA- and It-loaded RGD-LNCs (CsA + It RGD-LNCs) on surface expression of VEGF-R2 after an incubation period of 24 h relative to control (untreated cells). Cells were additionally treated with 10 ng/ml VEGF.

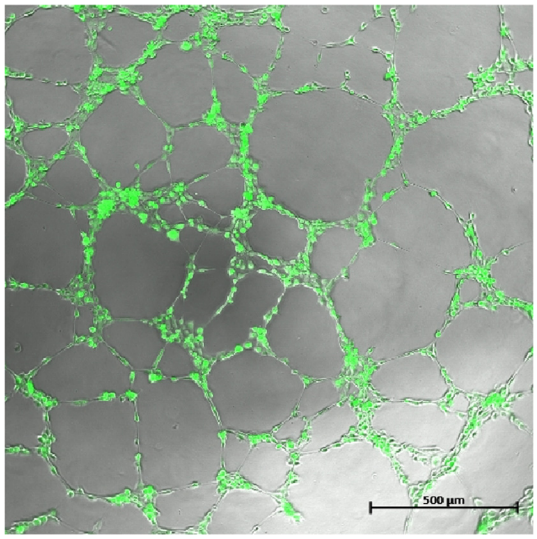

Fig. 7. Confocal Image (with a 5× objective, excited at 488 nm with an argon laser, emission recorded at 505 nm with a long pass filter) of Calcein-AM stained HDMECs, treated with BM (control) after an incubation period of 8 h at 37 °C.

binding to the $\alpha_v\beta_3$ integrin expressed by endothelial cells. However, we saw no anti-angiogenic effects for CsA- or CsA + It-loaded LNCs, contrary to the effects displayed by the free drugs, especially CsA. We hypothesize that this is due to the low intracellular escape of the poorly water-soluble drugs from the LNCs.

In the literature, very few studies can be found regarding the *in vitro* release or bioavailability of drugs from LNCs. LNCs are commonly used to overcome the poor water solubility of drugs like Ibuprofen [66], Quercetin, (–)-Epigallocatechin gallate [57], lipophilic radionuclides [67], methotrexate [68], ivermectin [69], Paclitaxel [70], Amiodarone [71], and antipsychotic drugs like promazine, chlorpromazine, thioridazine, trifluoperazine, triflupromazine, and chlorprothixene [38]. In one of the few studies that report drug release kinetics for LNCs, *in vitro* release was only observed for promazine and chlorpromazine, while very lipophilic drugs like thioridazine, trifluoperazine, triflupromazine, and chlorprothixene were not discharged from LNCs [38]. In the case of amiodarone, satisfactory release characteristics could only be achieved by pH adjustment and the addition of blank LNCs to the release medium

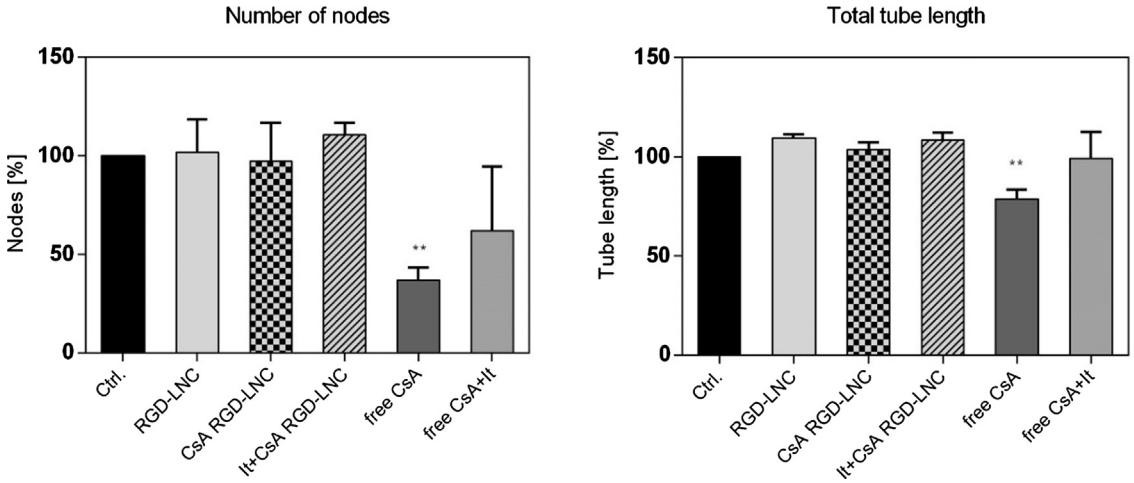

Fig. 8. Quantification of tube formation by HDMECs after treatment with free CsA (25 µg/ml), free CsA + It (1.0 + 0.1 µg/ml) or 0.6 mg/ml of RGD-LNCs, CsA-loaded RGD-LNCs (CsA RGD-LNC) or CsA- and It-loaded RGD-LNCs (It + CsA RGD-LNCs) in presence of 10 ng/ml VEGF, relative to control (untreated cells). Number of nodes and total tube length relative to control (untreated cells) was determined after an incubation period of 8 h.

as an acceptor phase [71]. In another study, in which ibuprofen was taken as a model drug and encapsulated in LNCs, first order release kinetics were observed [66]. A problem with this result is the low $logP_{Oct}$ value for ibuprofen of 1.2 [72] that hardly reflects a lipophilic drug.

In contrast to drug delivery applications where release is desired, the firm immobilization of lipophilic compounds in LNCs may be an advantage in some cases such as when dyes or radiolabels are used for diagnostic purposes. Highly lipophilic indocarbocyanines like DiD, DiI and DiO, for example, did not leach from the particles even when oil was used as a lipophilic acceptor phase [73]. Lipophilic ^{99m}Tc-oxine incorporated in the lipid core of LNCs remained inside the particles even when submitted to aggressive release conditions such as dialysis. This made the labeled nanoparticles an ideal tool to evaluate LNC biodistribution *in vivo* [74].

In summary, these results raise doubts as to whether it is possible to improve the intracellular bioavailability of poorly soluble drugs by the encapsulation into lipid nanoparticles. A definite advantage of the technology is that the drug can be dissolved in the lipid phase of a particle, allowing for perfect dispersion in an aqueous medium. That such particles can be taken up by cells has been proven in numerous studies [75]. However, what seems to be an advantage for the production of drug-loaded LNCs might be a handicap when it comes to intracellular drug release. Thus, it cannot be taken for granted that the encapsulated amount of drug corresponds to the amount of drug that is readily available inside cells. The active, available amount of drug seems to be dependent mainly on the drug-lipid interaction and the partitioning of the drug between the oily core of LNCs and the surrounding aqueous phase [38]. We should, however, not forget that dissolution is a time dependent process and that the kinetics of intracellular release must be considered as well. In our experiments, the time scale of observation was approximately 24 h which does not rule out the possibility that the drug might become available when observing release over longer time periods. Whether such slow kinetics would be able to elicit the desired biological effects, however, needs to be scrutinized on a case-by-case basis.

5. Conclusion

CsA- and CsA + It-loaded, RGD-grafted LNCs were prepared successfully. Even though RGD-LNCs showed excellent cell internalization properties, we were not able to achieve satisfactory biological effects with drug-loaded RGD-LNCs *in vitro* compared to free drug. This observed lack of efficacy can be explained by the poor intracellular availability of lipophilic drugs from LNCs. If this observation holds true for our drug-particle combination only or if it is a more general trend remains to be seen. As a result, the intracellular release of drugs from LNCs should be investigated more carefully in future studies. Such studies could clarify if the ease of drug encapsulation in LNCs comes at the expense of limited biological drug efficacy.

Acknowledgments

We thank Renate Liebl for her assistance in cell culture and Josef Kiermaier for his support with UHPLC-MS analytics. We also thank Katherine Fein for carefully revising this manuscript. This work was supported by Deutsche Forschungsgemeinschaft Grant GO565/18-1.

Appendix A. Supplementary material

Supplementary data to this article can be found online at https://doi.org/10.1016/j.ejpb.2019.03.007.

References

[1] N.T. Huynh, C. Passirani, P. Saulnier, J.P. Benoit, Lipid nanocapsules: a new platform for nanomedicine, Int. J. Pharm. 379 (2009) 201–209.
[2] B. Heurtault, P. Saulnier, B. Pech, A novel phase inversion-based process for the preparation of lipid nanocarriers, Pharm. Res. (2002) 875–880.
[3] H. Grossniklaus, R. Green, Choroidal neovascularization, Am. J. Ophthalmol. 137 (2004) 496–503.
[4] G.A. Peyman, J. Koziol, Age-related macular degeneration and its management, J. Cataract Refract. Surg. 14 (1988) 421–430.
[5] T. Murata, T. Ishibashi, A. Khalil, Y. Hata, H. Yoshikawa, H. Inomata, Vascular endothelial growth factor plays a role in hyperpermeability of diabetic retinal vessels, Ophthalmic Res 27 (1995) 48–52.
[6] L.P. Aiello, R.L. Avery, P.G. Arrigg, B.A. Keyt, H.D. Jampel, S.T. Shah, L.R. Pasquale, H. Thieme, M.A. Iwamoto, J.E. Park, H.V. Nguyen, L.M. Aiello, N. Ferrara, G.L. King, Vascular endothelial growth factor in ocular fluid of patients with diabetic retinopathy and other retinal disorders, N. Engl. J. Med. (1994) 1480–1486.
[7] J.-P. Tong, W.-M. Chan, D.T.L. Liu, T.Y.Y. Lai, K.-W. Choy, C.-P. Pang, D.S.C. Lam, Aqueous humor levels of vascular endothelial growth factor and pigment epithelium-derived factor in polypoidal choroidal vasculopathy and choroidal neovascularization, Am. J. Ophthalmol. 141 (2006) 456–462.
[8] M. Klagsbrun, S. Soker, VEGF/VPF: the angiogenesis factor found? Curr. Biol. (1993) 699–702.
[9] D.R. Senger, S.J. Galli, A.M. Dvorak, Tumor cells secrete a vascular permeability factor that promotes accumulation of ascites fluid, Sience (1983) 983–985.
[10] W.G. Roberts, G.E. Palade, Increased microvascular permeability and endothelial fenestration induced by VEGF, J. Cell Sci. (1995) 2369–2379.
[11] L.P. Aiello, E.A. Pierce, E.D. Foley, H. Takagi, H. Chen, L. Riddle, N. Ferrara, G.L. King, L.E. Smith, Suppression of retinal neovascularization in vivo by inhibition of vascular endothelial growth factor (VEGF) using soluble VEGF-receptor chimeric proteins, Proc. Natl. Acad. Sci. 92 (1995) 10457–10461.

[12] T. Kamba, B.Y.Y. Tam, H. Hashizume, A. Haskell, B. Sennino, M.R. Mancuso, S.M. Norberg, S.M. O'Brien, R.B. Davis, L.C. Gowen, K.D. Anderson, G. Thurston, S. Joho, M.L. Springer, C.J. Kuo, D.M. McDonald, VEGF-dependent plasticity of fenestrated capillaries in the normal adult microvasculature, American journal of physiology, Heart Circul. Physiol. 290 (2006) H560–76.
[13] M. Saint-Geniez, A.S.R. Maharaj, T.E. Walshe, B.A. Tucker, E. Sekiyama, T. Kurihara, D.C. Darland, M.J. Young, P.A. D'Amore, Endogenous VEGF is required for visual function: evidence for a survival role on müller cells and photoreceptors, PloS One 3 (2008) e3554.
[14] J.M. Rosenstein, J.M. Krum, New roles for VEGF in nervous tissue–beyond blood vessels, Exp. Neurol. 187 (2004) 246–253.
[15] K. Sayanagi, Transient choroidal thinning after intravitreal bevacizumab injection for myopic choroidal neovascularization, Clip. Experiment. Ophthalmol. (2011).
[16] J. Grunwald, E. Daniel, J. Huang, G. Ying, M. Maguire, C. Toth, G. Jaffe, S. Fine, B. Blodi, M. Klein, A. Martin, S. Hagstrom, D. Martin, Risk of geographic atrophy in the comparison of age-related macular degeneration treatments trials, Ophthalmology 121 (2014) 150–161.
[17] J.B. Evans, B.A. Syed, New hope for dry AMD? Nat. Rev. Drug Discov. 12 (2013) 501–502.
[18] C. Hernández, A. Simó-Servat, P. Bogdanov, R. Simó, Diabetic retinopathy: new therapeutic perspectives based on pathogenic mechanisms, J. Endocrinol. Invest. (2017).
[19] K. Hodivala-Dilke, alphavbeta3 integrin and angiogenesis: a moody integrin in a changing environment, Curr. Opin. Cell Biol. 20 (2008) 514–519.
[20] M. Friedlander, C.L. Thehsfeld, M. Sugita, M. Fruttiger, M.A. Thomas, S. Chang, D.A. Cheresh, Involvement of inegrins alphavbeta3 and alphavbeta5 in ocular neovascular diseases, Proc. Nat. Acad. Sci. (1996) 9764–9769.
[21] R.B. Brem, S.G. Robbins, D.J. Wilson, L.M. O'Rourke, Immunolocalization of integrins in the human retina, Invest. Ophthalmol. Vis. Sci. (1994) 3466–3474.
[22] S.G. Robbins, R.B. Brem, D.J. Wilson, L.M. O'Rourke, Immunolocalization of integrins in proliferative retinal membranes, Invest. Ophthalmol. Vis. Sci. (1994) 3475–3485.
[23] A. Arjonen, J. Alanko, S. Veltel, J. Ivaska, Distinct recycling of active and inactive β1 integrins, Traffic 13 (2012) 610–625.
[24] P. Caswell, J. Norman, Endocytic transport of integrins during cell migration and invasion, Trends Cell Biol. 18 (2008) 257–263.
[25] X. Liu, W. Cui, B. Li, Z. Hong, Targeted therapy for glioma using cyclic RGD-entrapped polyionic complex nanomicelles, Int. J. Nanomed. 7 (2012) 2853–2862.
[26] K. Markó, M. Ligeti, G. Mezo, N. Mihala, E. Kutnyánszky, E. Kiss, F. Hudecz, E. Madarász, A novel synthetic peptide polymer with cyclic RGD motifs supports serum-free attachment of anchorage-dependent cells, Bioconj. Chem. 19 (2008) 1757–1766.
[27] P. Rafiee, J. Heidemann, H. Ogawa, N.A. Johnson, P.J. Fisher, M.S. Li, M.F. Otterson, C.P. Johnson, D.G. Binion, Cyclosporin A differentially inhibits multiple steps in VEGF induced angiogenesis in human microvascular endothelial cells through altered intracellular signaling, Cell Commun. Signal. (2004) 1–22.
[28] B.A. Nacev, J.O. Liu, Synergistic inhibition of endothelial cell proliferation, tube formation, and sprouting by cyclosporin A and itraconazole, PloS One 6 (2011) e24793.
[29] C. Esposito, A. Fornoni, F. Cornacchia, N. Bellotti, G. Fasoli, A. Foschi, I. Mazzucchelli, T. Mazzullo, L. Semeraro, A. Dal Canton, Cyclosporine induces different responses in human epithelial, endothelial and fibroblast cell cultures, Kidney Int. 58 (2000) 123–130.
[30] Z.-M. Bian, S.G. Elner, V.M. Elner, Regulation of VEGF mRNA expression and protein secretion by TGF-beta2 in human retinal pigment epithelial cells, Exp. Eye Res. 84 (2007) 812–822.
[31] O. Strauss, The retinal pigment epithelium in visual function, Physiol. Rev. 85 (2005) 845–881.
[32] A. Carmo, J.G. Cunha-Vaz, A.P. Carvalho, M.C. Lopes, Effect of cyclosporin-A on the blood-retinal barrier permeability in streptozotocin-induced diabetes, Mediators Inflamm. 9 (2000) 243–248.
[33] B.A. Nacev, P. Grassi, A. Dell, S.M. Haslam, J.O. Liu, The antifungal drug itraconazole inhibits vascular endothelial growth factor receptor 2 (VEGFR2) glycosylation, trafficking, and signaling in endothelial cells, J. Biol. Chem. 286 (2011) 44045–44056.
[34] C.R. Chong, J. Xu, J. Lu, S. Bhat, D.J. Sullivan, J.O. Liu, Inhibition of angiogenesis by the antifungal drug itraconazole, ACS Chem. Biol. 2 (2007) 263–270.
[35] R. Giannarelli, A. Coppelli, M. Sartini, M. Aragona, U. Boggi, F. Vistoli, G. Rizzo, S. Del Prato, F. Mosca, P. Marchetti, Effects of pancreas-kidney transplantation on diabetic retinopathy, Transplant international official journal of the European Society for Organ, Transplantation 18 (2005) 619–622.
[36] V.C. Chow, R.P. Pai, J.R. Chapman, P.J. O'connell, R.D. Allen, P. Mitchell, B.J. Nankivell, Diabetic retinopathy after combined kidney-pancreas transplantation, Clin. Transplant. 13 (1999) 356–362.
[37] I.A. Pearce, B. Ilango, R.A. Sells, D. Wong, Stabilisation of diabetic retinopathy following simultaneous pancreas and kidney transplant, Br. J. Ophthalmol. (2000) 736–740.
[38] H. Nehme, P. Saulnier, A.A. Ramadan, V. Cassisa, C. Guillet, M. Eveillard, A. Umerska, Antibacterial activity of antipsychotic agents, their association with lipid nanocapsules and its impact on the properties of the nanocarriers and on antibacterial activity, PloS One 13 (2018) e0189950.
[39] A. Umerska, N. Matougui, A.-C. Groo, P. Saulnier, Understanding the adsorption of salmon calcitonin, antimicrobial peptide AP114 and polymyxin B onto lipid nanocapsules, Int. J. Pharm. 506 (2016) 191–200.
[40] C. Luschmann, J. Tessmar, S. Schoeberl, O. Strauss, C. Framme, K. Luschmann, A. Goepferich, Developing an in situ nanosuspension: a novel approach towards the efficient administration of poorly soluble drugs at the anterior eye, Eur. J. Pharm. Sci. 50 (2013) 385–392.
[41] M. Brinkley, A brief survey of methods for preparing protein conjugates with dyes, haptens and crosslinking reagents, Bioconj. Chem. 3 (2002) 2–13.
[42] T. Perrier, P. Saulnier, F. Fouchet, N. Lautram, J.-P. Benoît, Post-insertion into Lipid NanoCapsules (LNCs): from experimental aspects to mechanisms, Int. J. Pharm. 396 (2010) 204–209.
[43] T. Mosmann, Rapid colorimetric assay for cellular growth and survival: application to proliferation and cytotoxicity assays, J. Immunol. Methods 65 (1983) 55–63.
[44] T.M. Buttke, J.A. McCubrey, T.C. Owen, Use of an aqueous soluble tetrazolium/formazan assay to measure viability and proliferation of lymphokine-dependent cell lines, J. Immunol. Methods 157 (1993) 233–240.
[45] P.N. Dean, J.W. Gray, F.A. Dolbeare, The analysis and interpretation of DNA distributions measured by flow cytometry, Cytometry 3 (1982) 188–195.
[46] P. Pozarowski, Z. Darzynkiewicz, Analysis of Cell Cycle by Flow Cytometry, in: A.H. Schönthal (Ed.), Checkpoint Controls and Cancer: Volume 2: Activation and Regulation Protocols, Human Press, Totowa, N.J., 2004, pp. 301–311.
[47] I. Nicoletti, G. Migliorati, M.C. Pagliacci, F. Grignani, C. Riccardi, A rapid and simple method for measuring thymocyte apoptosis by propidium iodide staining and flow cytometry, J. Immunol. Methods 139 (1991) 271–279.
[48] R. Nunez, DNA measurement and cell cycle analysis by flow cytometry, Curr. Issues Mol. Biol. 3 (2001) 67–70.
[49] I. Arnaoutova, J. George, H.K. Kleinman, G. Benton, The endothelial cell tube formation assay on basement membrane turns 20: State of the science and the art, Angiogenesis 12 (2009) 267–274.
[50] K.L. DeCicco-Skinner, G.H. Henry, C. Cataisson, T. Tabib, J.C. Gwilliam, N.J. Watson, E.M. Bullwinkle, L. Falkenburg, R.C. O'Neill, A. Morin, J.S. Wiest, Endothelial cell tube formation assay for the in vitro study of angiogenesis, J. Visual. Exp. JoVE (2014) e51312.
[51] C.A. Schneider, W.S. Rasband, K.W. Eliceiri, NIH Image to ImageJ: 25 years of image analysis, Nat. Methods 9 (2012) 671 EP -.
[52] I. Zaghloul, R.J. Ptachcinski, G.J. Burckart, Blood protein binding of cyclosporine in transplant patients, clinical research: immunosuppressive, Drugs (1987) 240–242.
[53] K. De Beule, Itraconazole: pharmacology, clinical experience and future development, Int. J. Antimicrob. Agents (1996) 175–181.
[54] S.E.A. Gratton, P.A. Ropp, P.D. Pohlhaus, J.C. Luft, V.J. Madden, M.E. Napier, J.M. DeSimone, The effect of particle design on cellular internalization pathways, PNAS 105 (2008) 11613–11618.
[55] K. Kettler, K. Veltman, D. van de Meent, A. van Wezel, A.J. Hendriks, Cellular uptake of nanoparticles as determined by particle properties, experimental conditions, and cell type, Environ. Toxicol. Chem. 33 (2014) 481–492.
[56] P. Foroozandeh, A.A. Aziz, Insight into cellular uptake and intracellular trafficking of nanoparticles, Nanoscale Res. Lett. 13 (2018).
[57] A. Barras, A. Mezzetti, A. Richard, S. Lazzaroni, S. Roux, P. Melnyk, D. Betbeder, N. Monfilliette-Dupont, Formulation and characterization of polyphenol-loaded lipid nanocapsules, Int. J. Pharm. 379 (2009) 270–277.
[58] J. Choi, E. Rustique, M. Henry, M. Guidetti, V. Josserand, L. Sancey, J. Boutet, J.-L. Coll, Targeting tumors with cyclic RGD-conjugated lipid nanoparticles loaded with an IR780 NIR dye: In vitro and in vivo evaluation, Int. J. Pharm. 532 (2017) 677–685.
[59] S. Hirsjärvi, C. Belloche, F. Hindré, E. Garcion, J.-P. Benoît, Tumour targeting of lipid nanocapsules grafted with cRGD peptides, Eur. J. Pharm. Biopharm. Off. J. Arbeitsgemeinschaft fur Pharmazeutische Verfahrenstechnik e.V 87 (2014) 152–159.
[60] A. Paillard, F. Hindré, C. Vignes-Colombeix, J.-P. Benoit, E. Garcion, The importance of endo-lysosomal escape with lipid nanocapsules for drug subcellular bioavailability, Biomaterials 31 (2010) 7542–7554.
[61] K. Gupta, S. Kshirsagar, W. Li, L. Gui, S. Ramakrishnan, P. Gupta, P.Y. Lwa, R.P. Hebbel, VEGF prevents apoptosis of human microvascular endothelial cells via opposing effects on MAPK/ERK and SAPK/JNK signaling, Exp. Cell Res. 247 (1999) 495–504.
[62] W.J. Lamoreaux, M.E.C. Fitzgerals, A. Reiner, K.A. Hasty, S.T. Charles, Vascular endothelial growth factor increases release of gelatinase a and decreases release of tissue inhibitor of metalloproteinases by microvascular endothelial cellsin vitro, Microvasc. Res. 55 (1998) 29–42.
[63] A. Pardee, G1 events and regulation of cell proliferation, Science 246 (1989) 603–608.
[64] N. Ferrara, H.-P. Gerber, J. LeCouter, The biology of VEGF and its receptors, Nat. Med. 9 (2003) 669.
[65] I. Arnaoutova, H.K. Kleinman, *In vitro* angiogenesis: Endothelial cell tube formation on gelled basement membrane extract, Nat. Protoc. 5 (2010) 628.
[66] M.M.A. Abdel-Mottaleb, D. Neumann, A. Lamprecht, In vitro drug release mechanism from lipid nanocapsules (LNC), Int. J. Pharm. 390 (2010) 208–213.
[67] A. Béduneau, F. Hindré, A. Clavreul, J.-C. Leroux, P. Saulnier, J.-P. Benoît, Brain targeting using novel lipid nanovectors, J. Control. Release 126 (2008) 44–49.
[68] A. Boechat, C. Oliveira, A. Tarragô, A. da Costa, A. Malheiro, S. Guterres, A. Pohlmann, Methotrexate-loaded lipid-core nanocapsules are highly effective in the control of inflammation in synovial cells and a chronic arthritis model, Int. J. Nanomed. 10 (2015) 6603–6614.
[69] G.V.U. Gamboa, S.D. Palma, A. Lifschitz, M. Ballent, C. Lanusse, C. Passirani, J.P. Benoit, D.A. Allemandi, Ivermectin-loaded lipid nanocapsules: toward the development of a new antiparasitic delivery system for veterinary applications, Parasitol. Res. 115 (2016) 1945–1953.
[70] F. Lacoeuille, F. Hindre, F. Moal, J. Roux, C. Passirani, O. Couturier, P. Cales, J.J. Le Jeune, A. Lamprecht, J.P. Benoit, In vivo evaluation of lipid nanocapsules as a promising colloidal carrier for paclitaxel, Int. J. Pharm. 344 (2007) 143–149.

[71] A. Lamprecht, Y. Bouligand, J.-P. Benoit, New lipid nanocapsules exhibit sustained release properties for amiodarone, J. Control. Release 84 (2002) 59–68.
[72] H. Potthast, J.B. Dressman, H.E. Junginger, K.K. Midha, H. Oeser, V.P. Shah, H. Vogelpoel, D.M. Barends, Biowaiver monographs for immediate release solid oral dosage forms: Ibuprofen, J. Pharm. Sci. 94 (2005) 2121–2131.
[73] G. Bastiat, C.O. Pritz, C. Roider, F. Fouchet, E. Lignieres, A. Jesacher, R. Glueckert, M. Ritsch-Marte, A. Schrott-Fischer, P. Saulnier, J.-P. Benoit, A new tool to ensure the fluorescent dye labeling stability of nanocarriers: a real challenge for fluorescence imaging, J. Controll. Release Off. J. Controll. Release Soc. 170 (2013) 334–342.
[74] A. Cahouet, B. Denizot, F. Hindré, C. Passirani, B. Heurtault, M. Moreau, J.J. Le Jeune, J.P. Benoît, Biodistribution of dual radiolabeled lipidic nanocapsules in the rat using scintigraphy and γ counting, Int. J. Pharm. 242 (2002) 367–371.
[75] S. Hirsjärvi, S. Dufort, J. Gravier, I. Texier, Q. Yan, J. Bibette, L. Sancey, V. Josserand, C. Passirani, J.-P. Benoit, J.-L. Coll, Influence of size, surface coating and fine chemical composition on the in vitro reactivity and in vivo biodistribution of lipid nanocapsules versus lipid nanoemulsions in cancer models, Nanomed. Nanotechnol., Biol., Med. 9 (2013) 375–387.